Applied Radiation and Isotopes 115 (2016) 61–66

Contents lists available at ScienceDirect

Applied Radiation and Isotopes

journal homepage: www.elsevier.com/locate/apradiso

Moisture effect in prompt gamma measurements from soil samples

A.A. Naqvi [a,*], F.Z. Khiari [a], F.A. Liadi [a], Khateeb-ur-Rehman [a], M.A. Raashid [a], A.H. Isab [b]

[a] Department of Physics, King Fahd University of Petroleum and Minerals, Dhahran, Saudi Arabia
[b] Department of Chemistry, King Fahd University of Petroleum and Minerals, Dhahran, Saudi Arabia

HIGHLIGHTS

- Silicon, hydrogen and oxygen prompt gamma ray measurements from soil samples containing 0–14 wt% moisture (water) concentration.
- 14 MeV neutrons based PGNAA setup with $LaBr_3$:Ce gamma ray detector.
- With increasing moisture concentration decreasing intensity of Si and O prompt gamma rays.
- With increasing moisture concentration increasing intensity of H prompt gamma rays.
- Monte Carlo calculation of Si, H and O prompt gamma ray intensities from soil samples.
- Good agreement between the experimental and calculated results.

ARTICLE INFO

Article history:
Received 16 March 2016
Received in revised form
29 May 2016
Accepted 12 June 2016
Available online 14 June 2016

Keywords:
Silicon
Hydrogen and oxygen gamma ray intensity measurements
Soil samples with 0–14 wt% moisture concentration
14 MeV neutron based PGNAA setup with $LaBr_3$:Ce detector
Decreasing intensity of Si gamma ray with moisture
Increasing intensity of hydrogen with moisture
Monte Carlo calculation for gamma ray intensity from soil samples

ABSTRACT

The variation in intensity of 1.78 MeV silicon, 6.13 MeV oxygen, and 2.22 MeV hydrogen prompt gamma rays from soil samples due to the addition of 5.1, 7.4, 9.7, 11.9 and 14.0 wt% water was studied for 14 MeV incident neutron beams utilizing a $LaBr_3$:Ce gamma ray detector. The intensities of 1.78 MeV and 6.13 MeV gamma rays from silicon and oxygen, respectively, decreased with increasing sample moisture. The intensity of 2.22 MeV hydrogen gamma rays increases with moisture. The decrease in intensity of silicon and oxygen gamma rays with moisture concentration indicates a loss of 14 MeV neutron flux, while the increase in intensity of 2.22 MeV gamma rays with moisture indicates an increase in thermal neutron flux due to increasing concentration of moisture. The experimental intensities of silicon, oxygen and hydrogen prompt gamma rays, measured as a function of moisture concentration in the soil samples, are in good agreement with the theoretical results obtained through Monte Carlo calculations.

1. Introduction

Soil contamination is a major issue in environmental studies. There are several factors which contribute to soil pollution, but some of the major factors contributing towards soil contamination are industrial toxic waste discharge into the ground (Mulligan et al., 2001) and Petroleum hydrocarbons (PHC) contamination of soil surface (Atlas, 1981; Kirka et al., 2005). Prompt Gamma Neutron Activation Analysis (PGNAA) techniques have been successfully used to analyze hydrocarbon contents of bulk samples using 14 MeV Neutron beams (Drake et al., 1969; Doron et al., 2014; Defense Nuclear Agency Report # DNA 2716, 1972; Engesser and Thompson, 1967; Simakov et al., 1998; Falahat et al., 2012; Naqvi et al., 2013; Shultis et al., 2001; Wielopolski et al., 2011). In short, 14 MeV neutrons beams can be used to analyze bulk soil samples for environmental studies.

The presence of moisture in bulk samples causes problems in prompt gamma analysis of bulk samples utilizing 14 MeV neutron beams. Hydrogen contents of moisture in bulk samples act as a moderator for fast neutrons, thereby reducing the 14 MeV neutron flux in the sample. This results in a decrease in intensity of 14 MeV neutron-induced prompt gamma rays from the sample. This

* Corresponding author.
E-mail address: aanaqvi@kfupm.edu.sa (A.A. Naqvi).

http://dx.doi.org/10.1016/j.apradiso.2016.06.010
0969-8043/

requires a correction in the intensity of 14 MeV neutron-induced prompt gamma rays for the intensity loss due to sample moisture. This correction may be done by measuring the corresponding increase in intensity of thermal neutron-induced gamma rays from a specific element, say hydrogen contained in the same sample. These inverse trends in intensity variation of 14 MeV neutron- and thermal neutron-induced prompt gamma rays from a sample containing moisture may be used to correct for the moisture-dependent intensity loss of 14 MeV neutron induced prompt gamma rays in a sample following the standard Multiple Linear Regression (MLR) analysis techniques used in commercial on-line PGNAA gauges for correction of moisture effects in the samples.

A systematic study has been carried out to measure the intensity of 14 MeV neutron-induced 1.78 MeV silicon gamma rays, 6.13 MeV oxygen prompt gamma rays and 2.22 MeV hydrogen prompt gamma rays from a soil sample containing various moisture concentrations. The 2.22 MeV hydrogen prompt gamma rays are produced in the soil sample due to the capture of thermal neutrons in the hydrogen of the moisture added to the soil sample, while the thermal neutrons are produced in the sample due to moderation of incident 14 MeV neutrons from hydrogen in the moisture contents added to the soil sample. The study is described in the following sections.

2. Gamma ray intensity calculations from soil samples

The intensities of 1.78 MeV silicon, 6.13 MeV oxygen, and 2.22 MeV hydrogen prompt gamma rays were calculated from soil samples containing 0–15 wt% moisture using the general purpose MCNP4B2 code (Briesmeister , 1997). The calculations were carried for the 14 MeV neutron-based PGNAA setup shown in Fig. 1. The procedure used in the present study was similar to the one described earlier (Naqvi et al., 2013). For continuation's sake, it will be described briefly. The simulations were carried out for prompt gamma rays induced by 14 MeV neutrons inelastic scattering in bulk soil samples. The PGNAA setup mainly consists of a cylindrical polyethylene plastic sample container with 106 mm × 125 mm (diameter × height) dimensions. The sample container is placed at 0° angle with respect to the 14 MeV neutron beam and at a center-to-center distance of 70 mm from the 14 MeV neutron source. The neutron source was assumed to be point source. The empty polyethylene container has a mass of 96 g with a density of 0.92 g/cm^3. In the simulation study, the plastic container was modeled thereby resulting in non-zero hydrogen gamma ray counts for zero-moisture concentration. The density of dry soil was taken as 1.69 g/cm^3. A cylindrical 76 mm × 76 mm (diameter × height) $LaBr_3$:Ce detector, placed at a center-to-center distance of 125 mm from the sample, detects the gamma rays from the sample at an angle of 90° with respect to the 14 MeV neutron beam axis. The detector was shielded against 14 MeV neutrons and gamma rays through tungsten and lead shielding, respectively. For this simulation study, the sample was divided into sub-cells of 1 cm thickness. This allowed the transport of the neutrons and gamma rays of appropriate statistical weight to the next adjacent cell, without any loss.

In order to study prompt gamma ray production over the sample volume, 14 MeV neutrons as well as thermal neutron intensities were calculated over the sample diameter for 0–20% moisture concentration using the F5 tally of a point detector. Fig. 2 shows the 14 MeV and thermal neutrons intensity profiles over the sample diameter. The 14 MeV point source was located at x= −5.3 cm. The fast neutron data is shown with different symbols. The symbols are superimposed upon each other because the change in intensity of 14 MeV neutrons for various moisture concentrations is insignificant. The decrease in 14 MeV flux is mainly due to 1/distance^2 dependence of flux from the source. This is confirmed by the 1/distance^2 fit made to the 14 MeV neutron intensity data shown by the solid line. The calculated thermal neutron intensity is plotted with symbols connected with solid lines. The thermal neutron intensity shows a dependence upon radial distance as well moisture concentration. The thermal neutron intensity first increases with increasing radial distance from the source then reaches a maximum around the sample center and finally starts decreasing afterwards. The initial increase in thermal neutron intensity is due to increasing moderation of fast neutrons due to increasing moisture concentration. The decrease in thermal neutron intensity beyond the sample center is due to the loss of 14 MeV neutrons. Fig. 3 shows the thermal neutron intensity radial profile on an enlarged scale. The location of thermal neutron

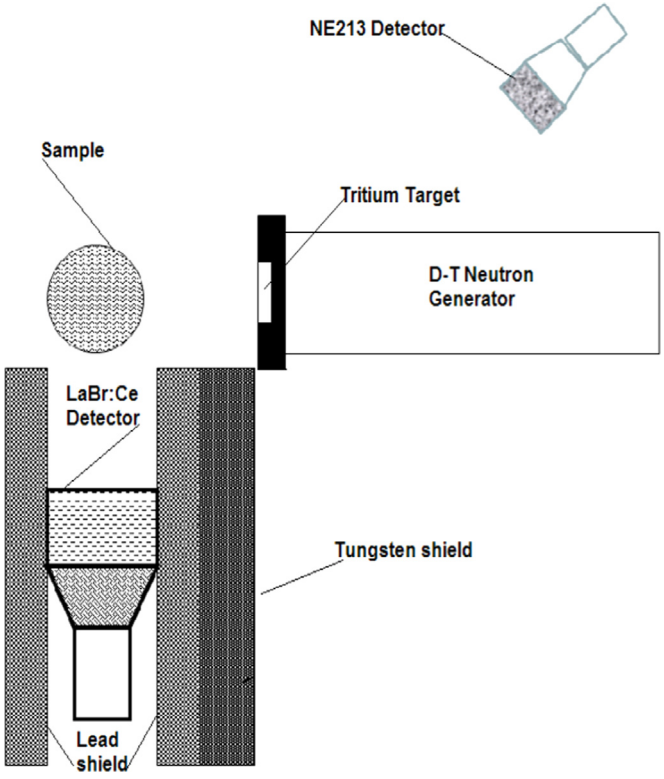

Fig. 1. Schematic of 14 MeV neutron-based setup used for analysis of soil bulk samples.

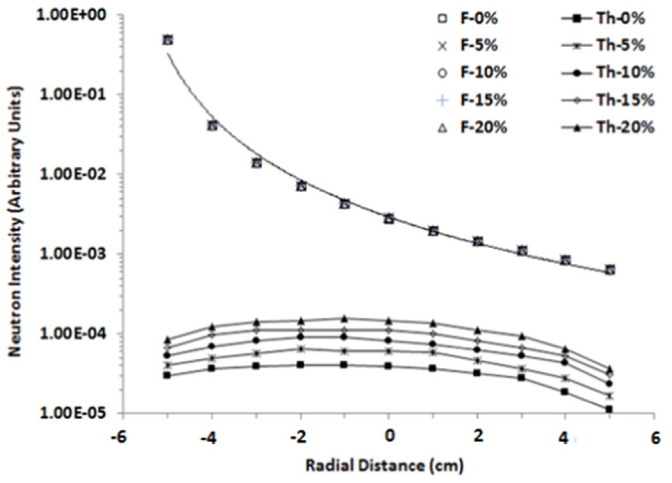

Fig. 2. Calculated intensity profile of 14 MeV and thermal neutrons plotted over the sample diameter for 0–20% moisture concentration (wt%).

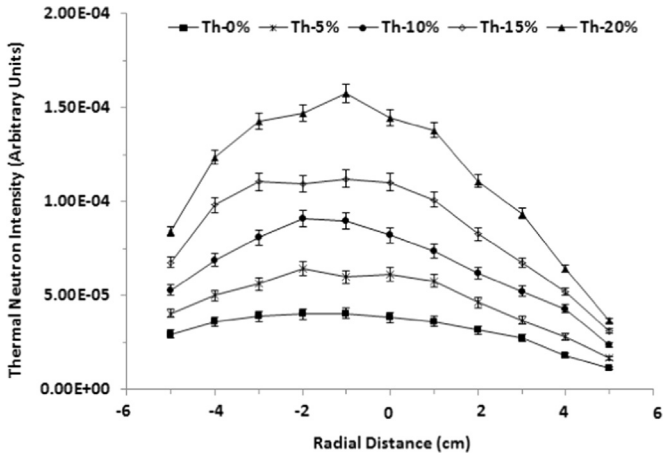

Fig. 3. Calculated intensity profile thermal neutrons plotted over the sample diameter for 0–20% moisture concentration (wt%).

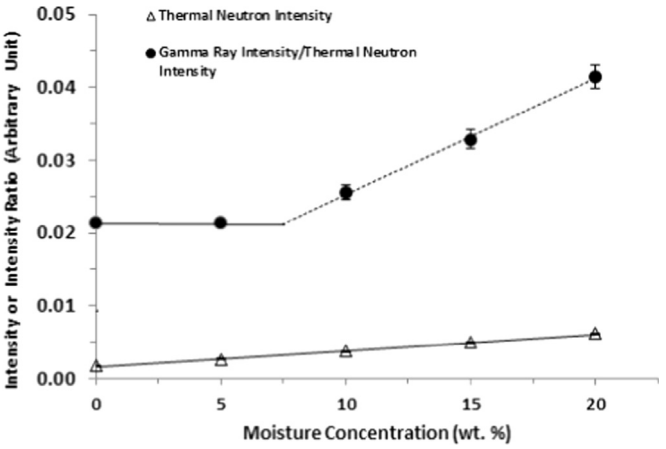

Fig. 4. Calculated thermal neutrons intensity as well as hydrogen gamma ray intensity/thermal neutron intensity ratio plotted as a function of moisture concentration (wt%).

intensity maximum is almost fixed around the center of sample diameter and is independent of moisture concentration. The thermal neutron intensity over the sample diameter increases with increasing moisture concentration.

The prompt gamma ray intensity was then calculated in the detector volume using the F4 tally. The chemical composition of the soil sample used in the simulation is given in Table 1. There was no hydrocarbon contamination in the sample which may moderate the 14 MeV neutrons. Water was added to a soil sample with a predetermined mass, thereby increasing the total sample mass. The soil samples were thoroughly mixed with water to achieve 0–15 wt% moisture concentration. Gamma ray intensities were calculated for 1.78 MeV silicon, 6.11 MeV oxygen, and 2.22 MeV hydrogen prompt gamma rays. The 2.22 MeV hydrogen gamma rays were produced due to capture of thermal neutrons in the hydrogen of the moisture in the sample. The thermal neutrons were produced due to moderation of 14 MeV neutrons in the sample.

In order to relate the variation in gamma ray intensity to change in thermal neutron flux due to added moisture, the thermal neutron and the hydrogen prompt gamma ray intensities were calculated inside the sample volume as a function of moisture concentration. Furthermore, the ratio of hydrogen gamma ray intensity to thermal neutron intensity was calculated. Fig. 4 shows the thermal neutron intensity as well as hydrogen gamma ray/thermal neutron intensity ratio plotted as a function of moisture concentration. The hydrogen gamma ray/thermal neutron intensity ratio curve should reflect the variation of gamma ray intensity as a function of moisture concentration only, excluding the effect of thermal neutron flux. The gamma ray/thermal neutron intensity ratio curve initially exhibits a plateau over a smaller moisture concentration range of 0–8% and then starts showing a linear dependence upon moisture concentration over 8–20% range, as shown by solid and dotted lines in Fig. 4. This trend is also clearly shown in Fig. 12, where experimental data is compared with calculated hydrogen gamma ray yield plotted as a function of moisture concentration. Since both the thermal neutron flux as well as hydrogen gamma ray/thermal neutron intensity ratio shown in Fig. 4 exhibits linear dependence upon moisture concentration beyond 8.0 wt%, it may be inferred that hydrogen gamma ray intensity will show a quadratic dependence upon moisture concentration beyond 8.0 wt%. This is confirmed by linear correlation among hydrogen gamma ray intensity and square of moisture concentration (wt%) plotted in Fig. 5.

Then intensity of 1.78 MeV silicon gamma rays and 6.13 MeV oxygen gamma rays were calculated as a function of moisture concentration in the soil samples. As the moisture concentration increases in the sample, the 14 MeV neutron flux decreases due to their increasing moderation in the sample. This results in decreasing intensities of the 1.78 MeV Si gamma rays and the 6.13 MeV O gamma rays with increasing moisture concentration in the soil sample, hence negative slope of the intensities of 1.78 MeV Si and 6.13 MeV O prompt gamma rays with respect to sample moisture concentration. Although a moisture increase causes an increase in oxygen concentration in the sample, but the decrease in 14 MeV flux is faster than the increase in oxygen concentration, thereby resulting in a net decrease in intensity of 6.13 MeV O gamma ray intensity.

Table 1
Chemical composition of dry soil sample used in the present study (Naqvi et al., 2009).

Composition	Constituents (wt%)
SiO_2	88.01
Al_2O_3	1.99
Fe_2O_3	0.28
MgO	0.57
CaO	3.18
Na_2O	0.44
K_2O	0.85
TiO_2	0.27

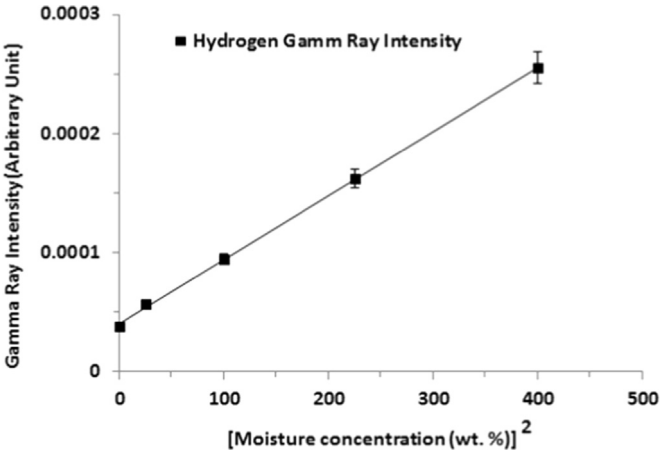

Fig. 5. Calculated hydrogen gamma ray intensity plotted as a function of [moisture concentration (wt%)]^2.

The slope of the gamma ray intensity as a function of moisture concentration is higher for silicon gamma rays (1.78 MeV) as compared to those of oxygen gamma rays (6.13 MeV). This might be due to a higher attenuation of lower energy silicon gamma rays as compared to the higher energy oxygen gamma rays in increasing moisture concentration. The increasing moderation of 14 MeV neutrons with increasing moisture concentration increases the thermal neutron flux in the sample. This results in an increase in the Intensity of 2.22 MeV hydrogen gamma rays from the soil sample. The 1.78 MeV Si prompt gamma rays and 2.22 MeV H prompt gamma rays have opposite trends in intensity variation with increasing moisture concentration in the soil sample. The results of Monte Carlo calculations have been shown in comparison with the experimental results.

3. Prompt gamma rays intensity measurements

The prompt gamma ray spectra from the soil samples and standards were recorded using the 14 MeV neutron based PGNAA setup described in the earlier studies (Naqvi, 2013). The setup is located at the end of the zero-degree beam line located in a reinforced concrete shielded room. The experimental setup has already been described earlier in Section 2. A pulsed beam of 14 MeV neutrons was produced via the T(d, n) reaction using a pulsed 110 keV deuteron beam with 200 ns pulse width and a frequency of 31 kHz. Pulsed ion beams are produced in the pre-acceleration stage of the KFUPM 350 keV accelerator using a diverter system. 200 ns pulses of 26 keV deuteron dc beams are produced by deflecting the dc deuteron beam across a water cooled aperture through a 2000 V voltage pulse of 200 ns duration and 31 kHz frequency, directly applied across the deflector plates of the diverter system.

The typical pulsed beam current of the accelerator was 60 μA averaged over the duty cycle of the 350 kV accelerator. The fast neutron flux from the tritium target was monitored using a cylindrical 76 mm × 76 mm (diameter × height) NE213 fast neutron detector, placed at a distance of 1.8 m from the target and making an angle of 130° with respect to the beam. The neutron flux spectrum was recorded through the proton recoil spectrum of the NE213 liquid scintillation detector during each run. In neutron spectroscopy, neutron detectors are operated at a specific discrimination level to suppress background neutrons and gamma ray signals. Therefore, the neutron detector signals are acquired in coincidence with a single channel analyzer whose SCA lower level is set at a fixed gamma-ray energy (also neutron energy). The neutron detector signals were acquired through a single channel analyzer, whose lower level was set at half-Cs pulse height bias that was electronically set by using the half-height of Compton edge spectrum of the ^{137}Cs gamma ray source.

The neutron spectrum counts were integrated for each run and were used later on for neutron flux normalization. The prompt gamma-ray spectra of the $LaBr_3$:Ce detector were recorded for a preset real time. The neutron and gamma ray detectors' spectra were acquired with a PC-based data acquisition system utilizing fast multichannel ADC buffer module 'ETHER-NIM 90E' manufactured by EG&G-ORTEC. The module utilizes Scintivision software to analyze the pulse height spectra of the detectors. Each detector spectrum was acquired in 512 channels.

For prompt gamma ray analysis, the soil samples were prepared by mixing 1863.8 g of dry soil with 5.1, 7.4, 9.7, 11.9 and 14.0 wt% water. The soil and water were thoroughly mixed together and soil completely absorbed the water. Then, the dry soil and as well as soil mixed with moisture samples were filled in plastic containers with 106 mm × 125 mm (diameter × height) dimensions. Empty and filled sample containers were then irradiated in the 14 MeV neutron-based PGNAA setup. The prompt gamma-ray data from the samples were acquired for 20–30 min. The typical dead-time of the pc-based data acquisition system was less than 1%. The empty container measurements were only repeated a few times because they had almost a constant spectrum. The empty container spectrum was used later on for background subtraction. The prompt gamma-ray data from the samples were acquired using the personal computer-based data acquisition system described earlier.

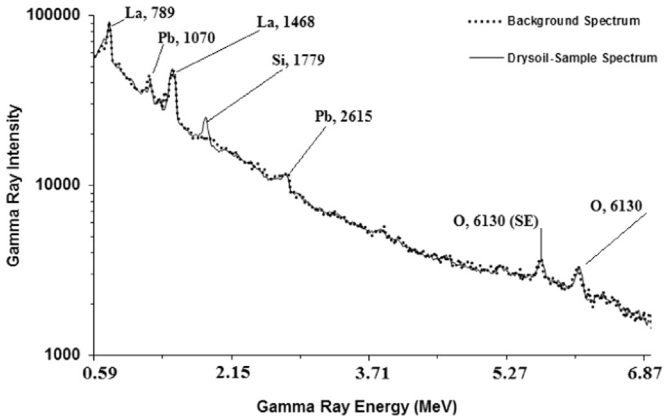

Fig. 6. Prompt gamma ray spectra of dry soil sample superimposed upon background spectrum and plotted over 0.59–6.87 MeV energy range.

3.1. Gamma ray intensity measurements from soil samples

Fig. 6 shows the spectrum of a dry soil sample superimposed upon a background spectrum taken with an empty container spectrum over 0.59–6.87 MeV range. The 1.78 MeV gamma ray peak from silicon and the 6.13 MeV peak from oxygen are quite prominent, along with the 789 and 468 keV intrinsic peaks of lanthanum and the 1.07 MeV as well as 2.62 MeV peak from lead shielding.

For the identification of high-energy silicon and oxygen gamma ray peaks in the soil sample spectrum, gamma ray peaks from samples with known elemental composition were recorded. For the identification of the silicon peak, the gamma ray spectrum was recorded from a silica fume sample. Silica fume has a 43.2 wt% concentration of silicon (Naqvi et al., 2009). For the oxygen peak identification in gamma ray spectrum, a water sample was used. Fig. 7 shows the prompt gamma spectra of silica fume and water samples superimposed over the 1.59–2.92 MeV range showing 1.78, 2.22, 2.09 and 2.62 MeV prompt gamma rays from silicon,

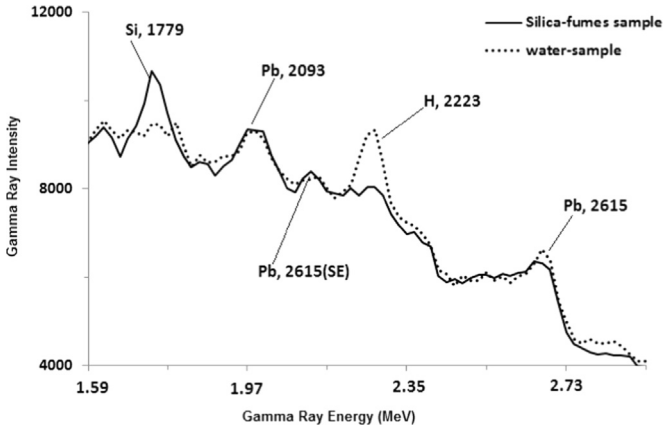

Fig. 7. Prompt gamma ray spectrum of silica fume sample superimposed upon water sample and plotted over 1.59–2.92 MeV energy range.

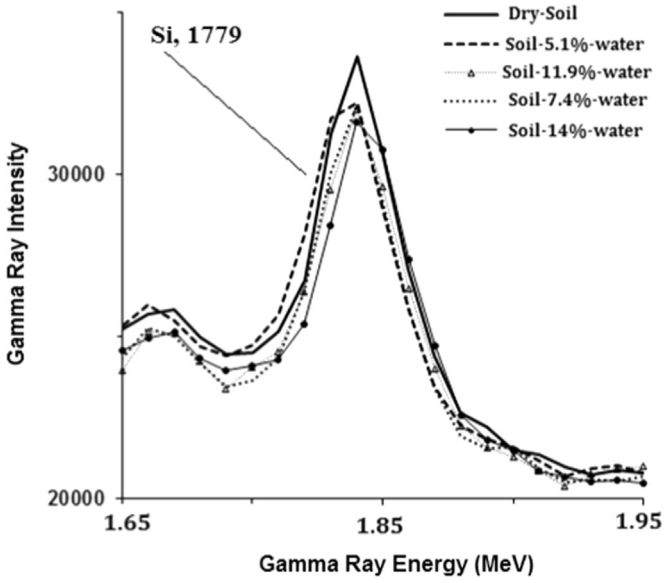

Fig. 8. Enlarged prompt gamma ray spectra of soil samples containing 5.1–14 wt% moisture superimposed upon dry soil sample plotted over 1.65–1.95 MeV energy range showing silicon peak.

hydrogen and lead (shielding material), respectively. The Single Escape peak (SE) corresponding to the 2.62 MeV full energy peak of lead is also shown in Fig. 7.

After the identification of silicon and oxygen prompt gamma ray peaks in the gamma ray spectrum, gamma ray spectra from dry soil and soil mixed with 5.1, 7.4, 9.7, 11.9 and 14.0 wt% water were recorded to study the effect of moisture using the PGNAA setup. In order to show the effect of moisture on silicon, hydrogen, and oxygen prompt gamma ray intensity, enlarged soil spectra containing 5.1–14 wt% moisture are superimposed upon a dry soil sample spectrum, as shown in Figs. 8–10. Fig. 8 shows enlarged soil spectra containing 5.1–14.0 wt% moisture over 1.65–1.95 MeV range showing 1.78 MeV gamma ray peaks from silicon. Effects of moisture on gamma ray intensity is quite significant and the intensity of 1.78 MeV Si gamma rays decreases with increasing moisture, with its maximum intensity observed for the dry soil

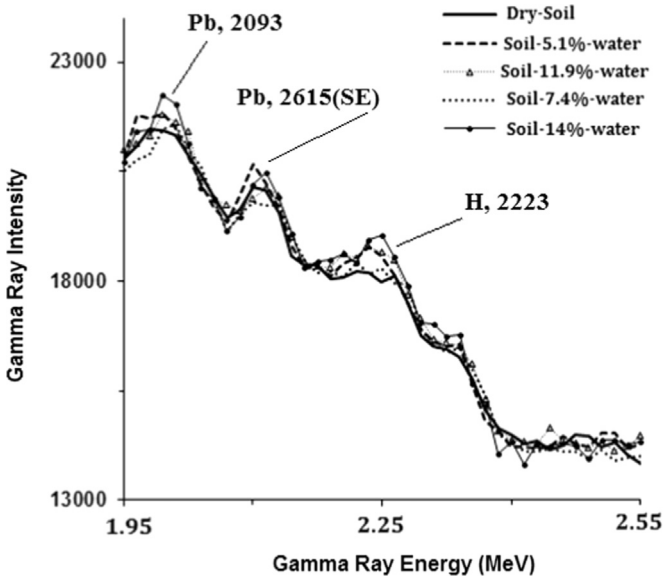

Fig. 9. Enlarged prompt gamma ray spectra of soil samples containing 5.1–14 wt% moisture superimposed upon dry soil sample and plotted over 1.95–2.55 MeV energy range, showing hydrogen and lead peaks.

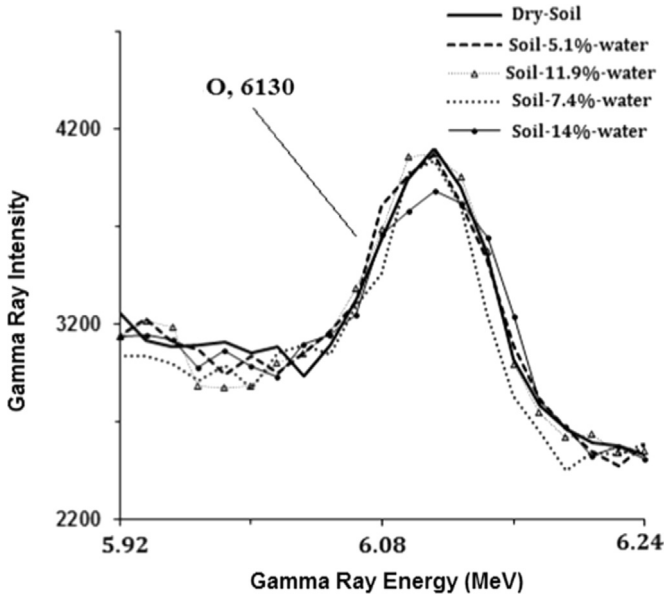

Fig. 10. Enlarged prompt gamma ray spectra of soil samples containing 5.1–14 wt% moisture superimposed upon dry soil sample and plotted over 5.92–6.24 MeV energy range, showing oxygen full energy peak.

sample.

Fig. 9 shows the 2.22 MeV hydrogen peak along with lead 2.09 MeV peak along with the single escape (SE) peak of lead 2.62 MeV full energy peak plotted over 1.95–2.55 MeV energy range for samples containing 5.1–14.0 wt% moisture. The increasing trend of the hydrogen peak intensity with increasing moisture concentration is quite prominent.

Fig. 10 shows the 6.13 MeV oxygen full energy peak on an enlarged scale plotted over 5.92–6.24 MeV energy range for samples containing 5.1–14.0 wt% moisture. The decreasing peak intensity of the 6.13 MeV oxygen full energy peak with increasing moisture concentration is clearly visible in Fig. 10.

Finally, the background was subtracted under the 1.78 MeV Si and 2.22 MeV hydrogen peaks spectrum by subtracting the background spectrum from the sample spectrum. For 6.13 MeV oxygen peaks the background under each peak was obtained by linear interpolation between two points, one on the lower energy side and the other on the higher energy side of the peak. The net counts under the peak were then obtained by integrating the counts in a window chosen on the background-subtracted peak. The net counts under each peak were further normalized to the integrated counts of the NE213 neutron monitor spectra to correct for any variation in neutron flux.

The corrected net counts for 1.78 MeV Si, 2.22 MeV H, and 6.13 MeV O peaks were plotted as a function of sample moisture concentration and are shown in Figs. 11 and 12. Fig. 11 shows the integrated counts of the 1.78 MeV silicon peak and 6.13 MeV oxygen peak plotted as a function of sample plotted as a function of sample moisture over 0–16 wt% concentration range. The fitted lines to the experimental data is the result of Monte Carlo calculations discussed in Section 2. Within the experimental uncertainties, the experimental results shown in Figs. 11 and 12 are in good agreement with the results of Monte Carlo calculation.

This study has provided useful results on moisture-dependent intensity variation of 1.78 MeV Si, 2.22 MeV H, and 6.13 MeV O prompt gamma rays from soil samples containing 5.1, 7.4, 9.7, 11.9 and 14.0 wt% water.

4. Conclusion

The effect of moisture on the intensity of 1.78 MeV Si, 2.22 MeV

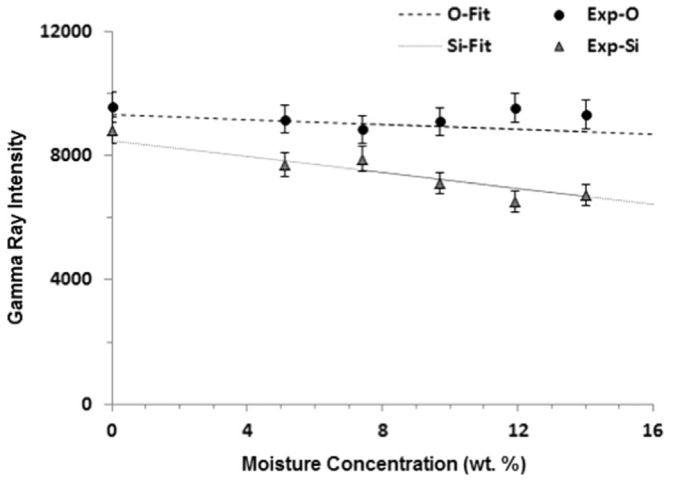

Fig. 11. Integrated intensity of 1.78 MeV silicon peak and 6.13 MeV oxygen peak from soil samples plotted as a function of moisture concentration of the soil samples over 0–16 wt% moisture concentration. The fitted line are results of Monte Carlo simulations.

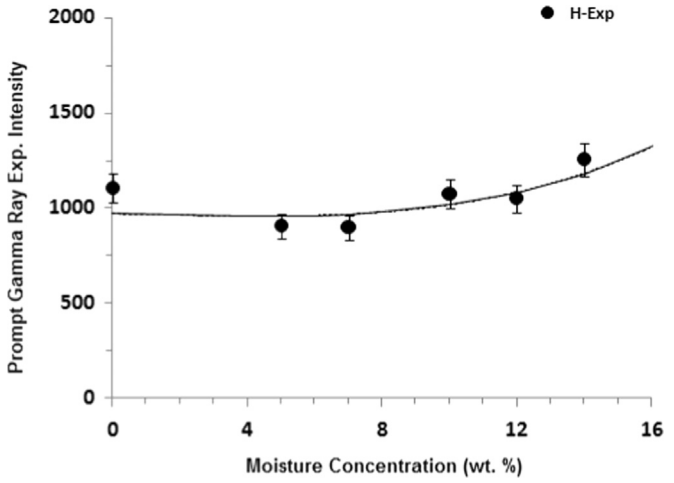

Fig. 12. Integrated intensity of 2.22 MeV hydrogen peak from soil samples plotted as a function of moisture concentration of the soil samples over 0–16 wt% moisture concentration. The fitted line is results of Monte Carlo simulations.

H, and 6.13 MeV O prompt gamma rays from soil samples containing 5.1, 7.4, 9.7, 11.9 and 14.0 wt% water was studied using a 14 MeV neutron-based PGNAA setup. Increasing moisture contents resulted in a decrease in the intensities of the 1.78 MeV Si and 6.13 MeV O gamma rays while it resulted in a corresponding increase in the intensity of the 2.22 MeV hydrogen prompt gamma rays from the soil samples. The experimental results are in good agreement with the results of Monte Carlo calculations. This study has provided useful results on moisture related intensity variations in 1.78 MeV Si and 2.22 MeV hydrogen prompt gamma rays.

Acknowledgement

This study has been funded through the National Science, Technology and Innovation Plan (NSTIP), project # 12-ENV2367-04. The support provided by the Department of Physics and the Department of Chemistry, King Fahd University of Petroleum and Minerals, Dhahran, Saudi Arabia, is also acknowledged.

References

Atlas, R.M., 1981. Microbial degradation of petroleum hydrocarbons: an environmental perspective. Microbiol. Rev. 45 (1), 180–209.

Briesmeister J.F. (Ed.), 1997. MCNP4B2 –A General Monte Carlo N-particles Transport Code. Los Alamos National Laboratory Report, LA-12625. Version 4C, Los Alamos National Laboratory Report, LA-12625-M.

Defense Nuclear Agency Report # DNA 2716, 1972. Neutron scattering and gamma ray production cross sections for N, O, Al, Si, CA and FE. Defense Nuclear Agency, Washington, DC 20305, USA.

Doron, O., Wielopolski, L., Mitra, S., Biegalski, S., 2014. MCNP benchmarking of an inelastic neutron scattering system for soil carbon analysis. Nucl. Instrum. Methods Phys. Res. Sect. A: Accel., Spectrom., Detect. Assoc. Equip. 735, 431–436.

Drake, D.M., Hopkins, J.C., Young, C.S., Die, H. Con, Sattler, A., 1969. Fast neutrons elastic and inelastic scattering from silicon. Nucl. Phys. A128, 209–218.

Engesser, F.C., Thompson, W.E., 1967. Gamma rays resulting from interactions of 14.7 MeV neutrons with various elements. J. Nucl. Energy 21, 487–507.

Falahat, S., Köble, T., Schumann, O., Waring, C., Watt, G., 2012. Development of a surface scanning soil analysis instrument. Appl. Radiat. Isot. 70, 1107–1109.

Kirka, J.L., Klironomosb, J.N., Leea, H., Trevorsa, J.T., 2005. The effects of perennial ryegrass and alfalfa on microbial abundance and diversity in petroleum contaminated soil. Environ. Pollut. 133, 455–465.

Mulligan, C.N., Yong, R.N., Gibbs, B.F., 2001. Remediation technologies for metal-contaminated soils and groundwater: an evaluation. Eng. Geol. 60 (1–4), 193–207.

Naqvi, A.A., Al-Matouq, Fares A., Khiari, F.Z., Isab, A.A., Raashid, M., Khateeb-ur-Rehman, 2013. Hydrogen, carbon and oxygen determination in proxy material samples using a $LaBr_3$:Ce detector. Appl. Radiat. Isot. 78, 145–150.

Naqvi, A.A., Garwan, M.A., Maslehuddin, M., Nagadi, M.M., Al-Amoudi, O.S.B., Khateeb-ur-Rehman, Raashid, M., 2009. Prompt gamma analysis of fly ash, silica fume and Superpozz blended cement concrete specimen. Appl. Radiat. Isot. 67, 1707–1710.

Shultis, J. Kenneth, Khan, F., Letellier, B., Fawa, Richard E., 2001. Determining soil contamination profiles from intensities of capture-gamma rays using above-surface neutron sources. Appl. Radiat. Isot. 54, 565–583.

Simakov, S.P., Pavlik, A., Vonach, H., Hlavac´, S., 1998. Status of experimental and evaluated discrete gamma-ray production at En = 14.5 MeV. IAEA Nuclear Data Section, Final Report of Research Contract 7809/RB,/http://www-NDS.IAEA.Org/reports-new/indc-reports/indc-ccp/indc-ccp-0413.pdf.

Wielopolski, L., Chatterjee, A., Mitra, S., Lal, R., 2011. In situ determination of soil carbon pool by inelastic neutron scattering: comparison with dry combustion. Geoderma 160, 394–399.